

Actin cytoskeletal organization in human osteoblasts grown on different dental titanium implant surfaces

M. Salido¹, J.I. Vilches², J.L. Gutiérrez² and J. Vilches¹

¹Department of Histology, School of Medicine, University of Cadiz, Spain and

²Department of Oral Surgery, School of Dentistry, University of Seville, Spain

Summary. The understanding of the cellular basis of osteoblastic cell-biomaterial interaction is crucial to the analysis of the mechanism of osseointegration. Cell adhesion is a complex process that is dependent on the cell types and on the surface microtopography and chemistry of the substrate.

We have studied the role of microtopography in modulating cell adhesion, *in vitro*, using a human osteoblastic cell line for the assessment of actin cytoskeletal organization. Through application of CLSM combining reflection and fluorescence, 2D or 3D images of cytoskeleton were obtained.

On smooth surfaces, Ti CP machined, predominantly planar bone cells with an axial ratio of 1.1 were randomly oriented, with stress fibers running in all directions, and thin filopodia.

On TiCP Osseotite[®] surfaces the osteoblastic cells conformed to the irregular terrain of the substrate with focal adhesion sites only established on the relative topographical peaks separated for a longer distance than in the machined surface, and defined wide lamellopodia and long filopodia, with enhanced expression of stress fibers, forming large clear focal contacts with the rough surface. The cytoskeletal organization of cells cultured on rough titanium supports an active role for the biomaterial surface in the events that govern osteoblastic cell adhesion. The results enforce the role of the rough substrate surface in affecting osteoblastic cell adhesion and provide valuable information for the design of material surfaces that are required for the development of an appropriate osteogenic surface for osteoblastic anchorage, compared to machined surface, in dental implants.

Key words: Osteoblasts, Cytoskeleton, Dental implants, Titanium, Microtopography

Introduction

Biomedical materials may be used for permanent implantation into the human body or as a temporary support for cells and tissues. In both cases, the aim is to tailor the surfaces to provide chemical and physical cues to guide differentiation and assembly of cells to form tissue or to become biocompatible with the surrounding tissue (Diener et al., 2005). Establishing and maintaining mature bone at the bone-device interface is critical for the long term success of prosthesis. Poor cell adhesion to orthopaedic and dental implants results in implant failure (Zreiqat et al., 2005). In this sense, understanding the cellular basis of osteoblastic cell-biomaterial interaction is crucial for the analysis of the mechanism of osseointegration, a requirement of long-term orthopaedic implant stability (Shah et al., 1999). Osseointegration can be defined morphologically as direct contact of the bone tissue and the implant surface, that is, an initial close apposition of bone and long-term stable bone ingrowth to the biocompatible surface (Shah et al., 1999; Papalexiou et al., 2004). Cell adhesion, spreading and signalling are complex processes that are dependent on the cell types, the maturation state of the cells, and on the surface microtopography and chemistry of the substrate with which the cells interact. These events regulate a wide variety of biological functions including cell growth, cell migration, cell differentiation, extracellular matrix synthesis, and tissue morphogenesis that are dependent on cytoskeletal organization to a great extent (Anselme, 2000; Lange et al., 2002; Boyan et al., 2003; Jayaraman et al., 2004; Lenhart et al., 2005).

The term "adhesion" in the biomaterial domain covers different phenomena. First, the attachment phase which occurs rapidly and involves short-term events like physicochemical linkages between cells and materials involving ionic forces, van der Waals forces, etc. The adhesion phase occurs in the longer term and involves biological molecules, such as cell membrane proteins, ECM proteins, and cytoskeleton proteins which interact together to induce signal transduction. This signal transduction, thus, promotes the action of transcription

factors and consequently regulation of gene expression. The sites of adhesion between tissue cultured cells and substrate surfaces are called focal contacts, closed junctions where the distance between the substrate surface and the cell membrane is between 10-15 nm. The external faces of focal contacts present specific receptor proteins such as integrins. On the internal face, some proteins like talin, paxillin, vinculin and tensin are mediating interactions between actin filaments and membrane receptor proteins, integrins (Zigmond, 1996; Anselme, 2000; Pierres et al., 2002)

Owing to the suitable physical properties and good biocompatibility, commercially pure titanium has been used as a successful and widespread material in various dental and orthopaedic applications, as well as titanium alloy (Brånemark et al., 1983; Bächle and Kohal, 2004; Zreiqat et al., 2005). The surfaces of currently available endosseous dental implants range from relatively smooth machined surfaces to those roughened by coating, abrasion or blasting, acid etching or a combination of these techniques (Mustafa et al., 2001; Linez Bataillon et al., 2002; Ronold et al., 2003a,b; Al Nawas and Gotz, 2003; Rodríguez-Rius and Garcia, 2003). In contrast to *in vivo* implant experiments, cell culture studies provide a useful tool for investigations because cell and matrix interactions with alloplastic material surfaces can be evaluated in detail (Bächle and Kohal, 2004). Culture models allow more controlled conditions, especially at a cellular level. Processes, such as cell attachment, motility, proliferation, and protein biosynthesis can be investigated.

To understand how microtopography modulates cell adhesion, in the present study we have developed an *in vitro* model using the human osteoblastic cell line NHOst[®] to study actin cytoskeletal organization during the initial phases of the adhesion process to different titanium implant surfaces, prepared as disks for *in vitro* manipulation. Prior to cell seeding, the quality control of implant devices was carried out using scanning electron microscopy and X ray microanalysis of surfaces in order to achieve three important goals: to determine the exact disk composition, to discard those disks that could be "contaminated" by cytotoxic compounds and finally to ensure that topography was homogeneous throughout the disks surface in both groups. Through application of high-resolution confocal laser scanning microscopy (CLSM) combining reflection and fluorescence principles, two -2D- or three dimensional -3D- images and a series of cytoskeleton and cells growing *in vitro* on 3D scaffolds can be obtained. Furthermore, confocal microscopy uses laser light to activate fluorescent substances, focusing the laser at the pre-established depth for the specimen, obtaining clear images. Successive images in different planes of the same specimen can be obtained for the reconstruction of 3D images. Thus, the dynamics of a physiological process, as is the case for the initial phases of osseointegration, can be determined. We have, thus, used this information to reconstruct the three-dimensional interface between

the osteoblastic cells and the implant surface.

Materials and methods

Test substrates

Prefabricated 2 cm x 1.5 mm disks were kindly provided by 3i (Palm Beach Gardens, USA). Ti-CP machined, and the dual thermo-acid etching Ti-CP-Osseotite[®] disks were used for the experiments. The surface features of the disks as well as their ionic composition were assessed by a Philips Quanta 200 scanning electron microscope equipped with a Phoenix EDS energy-dispersive X-ray microanalysis system at 20 kV, spot mode with a working distance (WD) of 9.9 mm. Spot was set at 4.5 for the machined disks and at 2.5 for the Osseotite[®] disks. Each spectrum was acquired for 200 seconds.

Cell culture

Norman human osteoblastic NHOst[®] cells (Cambrex, Walkersville, MD, USA) were seeded at a density of 5000 cells/cm² and incubated in Osteoblast Growing Medium, OGM, (Cambrex, Walkersville, MD, USA) containing 10% fetal bovine serum (Cambrex, Walkersville, MD, USA), 1% gentamycin sulphate/amphotericin B (Cambrex, Walkersville, MD, USA) and 1% ascorbic acid (Cambrex, Walkersville, MD, USA), as recommended by suppliers, at 37°C and 5% CO₂ until the experiments were started. Growth medium was changed every day after seeding. Before the cells became 80% confluent they were subcultured with 2 ml of 0.25 mg/ml trypsin EDTA warmed to 37°C (Cambrex, Walkersville, MD, USA) after rinsing with 5 ml HEPES-BSS (Cambrex, Walkersville, MD, USA) at room temperature. Once cells were detached, trypsin EDTA was neutralized by adding 4 ml of trypsin neutralizing solution (Cambrex, Walkersville, MD, USA). Harvested cells were seeded on the different disks at a density of 5000 cells/cm² and immunostained after 48 h. Growth medium was changed every day until the experiment was finished. NHOst cells are assured for experimental use for ten population doublings, which were not exceeded during the assay.

Before use, the disks were immersed in 100% ethanol for 10 min, air dried, and exposed under u.v. light for 30 min on each side, and finally rinsed in endotoxin free phosphate buffered solution (Ku et al., 2002), and deposited on small sterile Petri dishes prior to cell seeding. Tissue culture Willco[®] (Leica Microsystems, Darmstadt, Germany) plates with glass bottom were used as the control surface.

Cell morphology and spreading

Cells were routinely examined with the phase contrast microscope after seeding and changes in cell morphology, as well as alignment and initial adhesion

phase to surfaces were assessed prior to confocal examination.

Immunohistochemistry and cytoskeletal organization

Cells were passaged and cultured at a density of 5000 cells/ cm² on the different test surfaces. At the end of the specific culture time, cells were washed twice with prewarmed phosphate-buffered saline, (PBS), pH 7.4, and fixed with 3.7% paraformaldehyde (PFA) solution in PBS for 10 min. at room temperature and washed twice with prewarmed PBS. The cells were then permeabilized with 0.1% Triton x-100 (Sigma, St Louis, Missouri, USA) for 5 min and washed twice with prewarmed PBS. To reduce non-specific background staining 1% bovine serum albumine (BSA) in PBS was added to the surfaces for 20 min and immunostained for 20 min with rhodamine phalloidin, 12.5 μ l of methanolic stock solution (Sigma, St Louis, Missouri, USA) in 500 μ l PBS for each sample. Staining solution was discarded and disks were then rinsed with prewarmed PBS three times prior to mounting with vectashield[®] (Vector Labs. Burlingame CA, USA) in one holed (0.17 mm) polycarbonate slides designed in our laboratory and fabricated by means of control precision systems (Mecaprec, Cadiz, Spain)

Confocal examination

The cells and disks were simultaneously visualized using a Leica TCS-SL confocal microscope equipped with a 63.0x1.30 glycerol objective allowing simultaneous acquisition of rhodamine phalloidin staining of actin cytoskeleton (excitation 554 nm/emission 573 nm) and surface reflectance. Four isolated disks were analyzed in each group for topographical information, and four disks with cells growing on them were analyzed for each group to assess surface influence on cytoskeletal organization and cell morphology. At least 50 cells per disk were analysed.

Images were collected and processed for the quantitative analysis using the imaging software provided by the Leica TCS SL system. Profilometric studies, for the quantification of maximal and minimal values in surface profile, distance between peaks in each surface, width of grooves and valleys, and axial ratio of the cells growing on the different surfaces were assessed. All samples were exposed to laser for a time interval not higher than 5 min to avoid photobleaching. The excitation beam splitter selected was a DD 488/543. The laser was set to the lowest power that was able to produce a fluorescent signal. Maximum voltage of photomultipliers was used to decrease the required laser power as much as possible, the lowest voltage being 279.3 V and the highest voltage 778.7 V. Offset was maintained at 0. A pinhole of 1 Airy unit was used. Images were acquired at a resolution of 512x512, with a mean voxel size of 209.20 nm. Series were acquired in the xyz mode.

Statistical analysis

Means and standard deviations (SD) were calculated for descriptive statistical documentation. The Students T-test was applied for analytical statistics. A value of $p \leq 0.05$ was considered significant.

Results

Surface topography and composition

Scanning electron microscopy

Scanning electron microscopy of Ti- CP machined and Ti -CP- Osseotite[®] disks revealed specific differences that may determine cellular behaviour. As shown in Figure 1, the machined TiCP disks present a surface with parallel valleys, likely the result of machining, separating concentric rings with striated surface (Fig. 1). In contrast, TiCP Osseotite[®] disks show an irregular surface, with a marked porosity, mainly composed of spherulae, with aleatorily disposed concavities, and extremely variable distance between peaks (Fig. 1).

Confocal examination of surfaces

When samples were examined in the reflection mode of the confocal microscope, the machined surface revealed, as expected, a quite regular planar surface, with parallel grooves caused by the waviness inherent to the machining operation (Fig. 2) and the consequent embossed ring patterned surface with a small groove on top. The profilometric measurement resulted in a minimum value of 1.2 μ m for the depth of the valleys and a maximum value of 4.15 μ m for the top of the embossed structure. (Fig. 2E) The mean distance between tops reached 18.28 μ m, the mean width for the valleys was 2.85 μ m, the mean value found for the groove on top of each embossed ring was 1.51 μ m. (Fig. 2B, c,d,e) As shown in the figure (Fig. 3), Ti CP Osseotite[®] disks showed a marked increase in the surface roughness with prominent peaks and caves, some of them with well defined contours and some others forming a wide trabecular surface with randomly distributed peaks. The distance between peaks, consequently, was highly variable, with values ranging from 24.45 μ m up to 183.67 μ m (Fig. 3B, c). The mean diameter of the caves was found to be largely variable, ranging from 8.01 and 39.27 μ m. As revealed in the profilometric study, (Fig. 3E) this pattern notably increased the mean roughness of the surface that showed a minimum value of 1.9 μ m in depth and a maximum peak value of 8.79 μ m.

Energy dispersive X ray microanalysis

Measurement of the chemical composition with EDS did not provide any discrimination between the surfaces,

as it simply detected titanium and oxygen in both groups and no cytotoxic compounds were identified either in TiCP machined or in Ti CP Osseotite[®] surfaces (Fig. 4).

Phase contrast examination

Cells grown on microplates started to adhere to substrate after one hour culture. In the first minutes cells started flattening. After 10 minutes, the alignment phase became evident and osteoblasts started to face the disk

surface. After three hour culture cells started to spread and after twenty four hours culture, osteoblasts had started to align with respect to the disks and appeared elongated, flat and attached to the surfaces (Fig. 5).

Confocal examination of cell morphology

CLSM image combining the fluorescence and reflection modes helped us to illustrate cell-disk interaction and to demonstrate that osteoblasts assume

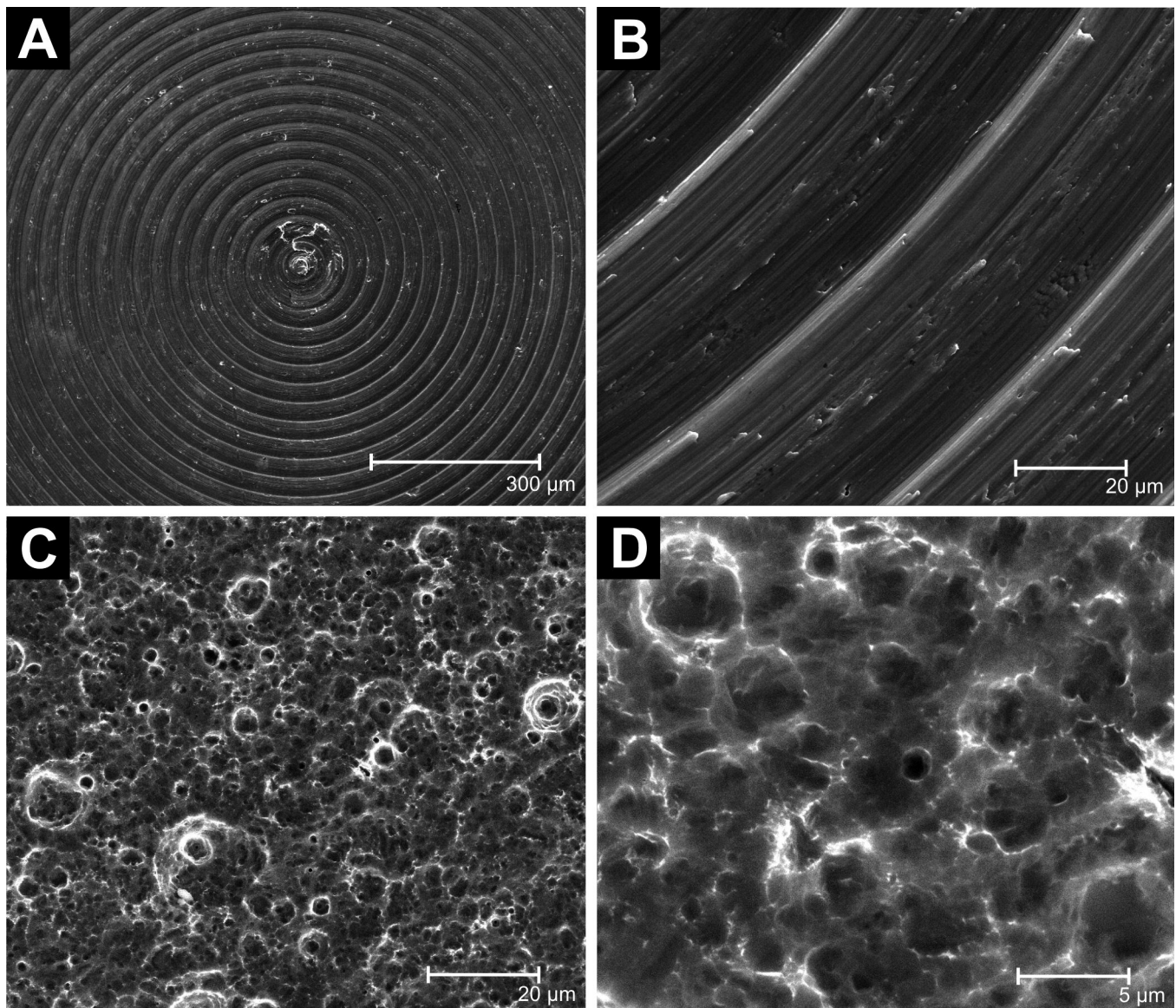


Fig. 1. Scanning electron microscopy of the surface morphology of 2 cm x 1.5 mm titanium test disks. **A.** TiCP machined surface contains parallel grooves that determine a relatively smooth surface. x 250. **B.** At higher magnification, the surface of TiCP machined disk appeared to have a homogeneous pattern with evenly distributed grooves and elevations. x 1,000. **C.** TiCP Osseotite[®] disks showed a markedly irregular surface with numerous crater-like structures. x 250. **D.** At higher magnification the TiCP Osseotite[®] surface showed randomly distributed cavities and borders. x 1000

Microtopography and cytoskeleton

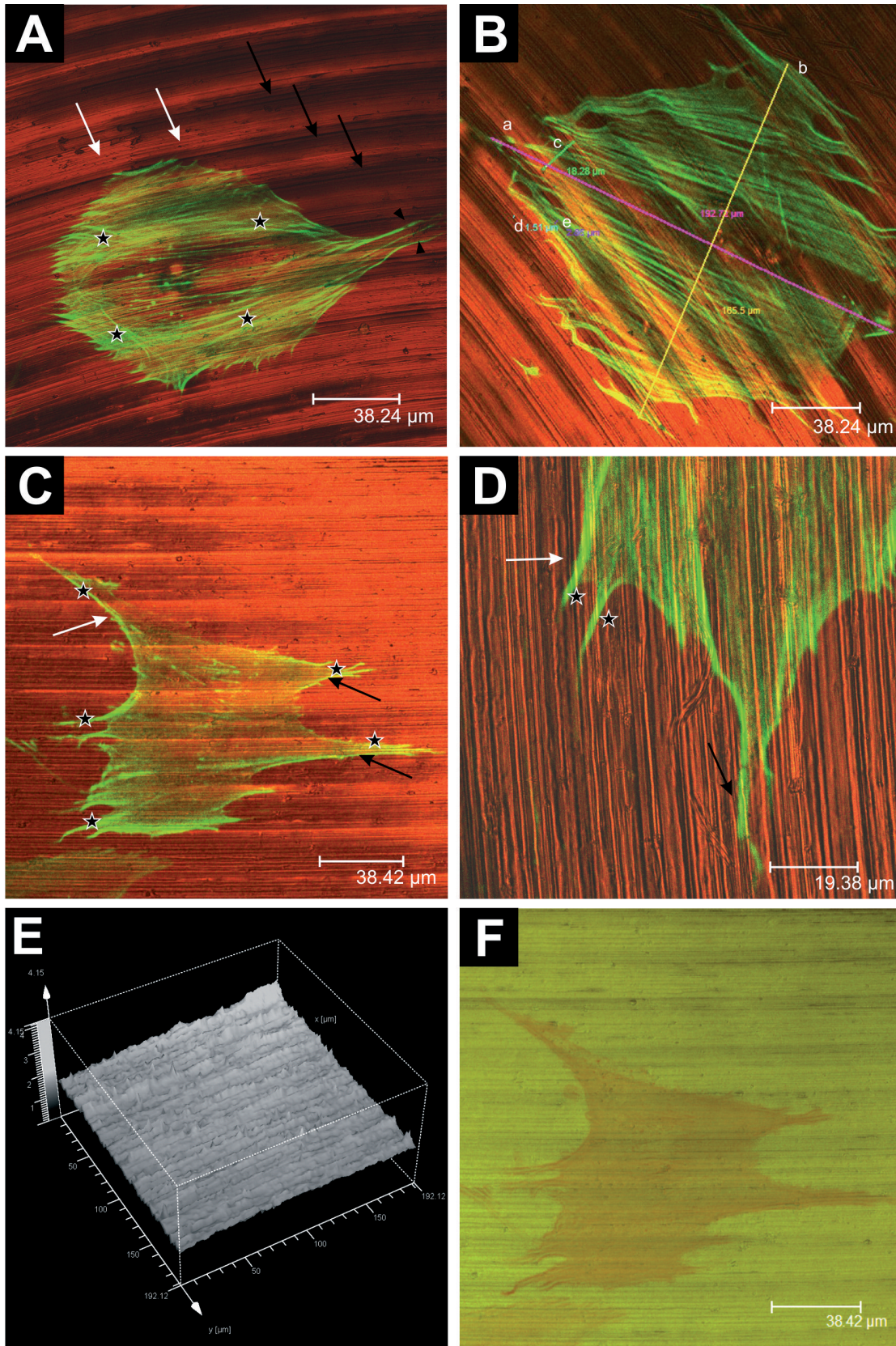


Fig. 2. CLSM image combining the fluorescence and reflection modes to illustrate cell-disk interaction in a TiCP machined disk. **A.** The machined surface, in red, contains parallel grooves (black arrow) that determined a concentric pattern of embossed rings (white arrow). Phalloidin stained for actin, in green, the cell adopted a largely radial morphology and anchored to the surface through long filopodia (arrowhead) with stress fibers running in all directions (*). $\times 63$. Zoom 1.00 **B.** At higher magnification, stress fibers (green) appeared to cross over the grooves (in red, disk surface) in non oriented cells. Marked with a, b the main axis of the cell that determined the axial ratio around 1.1. Marked with c, d, e, measurements for surface topography, as described in the text. $\times 63$. Zoom 1.64 **C.** Representative image of a NHOst cell anchored to the machined surface through long dendritic filopodia (black star) both along the grooves of the surface (black arrow) or crossing over them in a perpendicular way (white arrow) showed in **D**, at higher magnification. **C.** $\times 63$, Zoom 1; **D.** $\times 63$, Zoom 2.64. **E.** Topographical (3D) profilometric image of TiCP machined surface by confocal microscopy. **F.** Topographical (2D) reconstruction of a 3D series obtained with the CLSM, showing the distribution of stress fibers (red) in a flat NHOst cell growing on the machined surface (green). $\times 63$. Zoom 1.

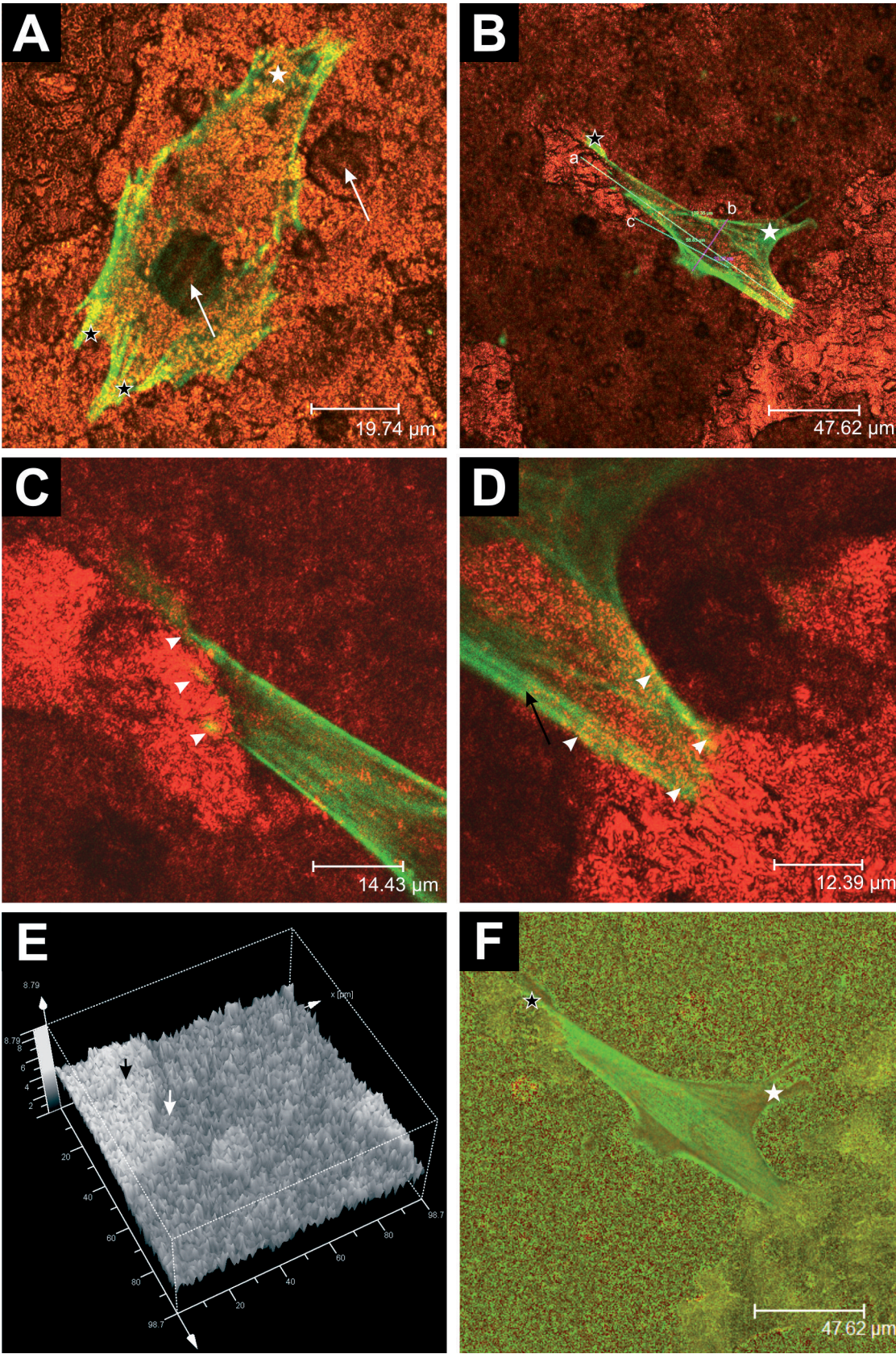


Fig. 3. CLSM image combining the fluorescence and reflection modes to illustrate cell-disk interaction in a TiCP Osseotite® disk. **A.** TiCP Osseotite® disks (in red) showed a marked increase in the surface roughness with prominent peaks and caves (white arrow). In this case, the cell (green) appeared to be adapted to a relatively regular surface, which allowed spreading by means of the emission of wide lamellopodia (white star) and also dendritic filopodia (black star). x 63.0, Zoom 2.41. In contrast, in **B**, the surface presented deeper valleys and more randomly distributed peaks than is the case for **A**. The cells, thus, presented an increasingly polarised spreading with emission of either wide lamellopodia (white star) or long filopodia (black star). Marked with a, b the main axis of the cell that determined the axial ratio around 3.5. Marked with c, the representative distance between peaks, as described in the text. x 63.0, Zoom 2.41. In **C**, with a zoom of 3.30, the focal adhesion sites, in yellow, in the apical part of the cell determined by contact of the actin stress fibers with the surface peaks are marked with white arrowheads. x 63.0. **D** shows at higher magnification, the yellow basal focal contacts (arrowhead) established between stress fibers (black arrow) and surface peaks. x 63.0, zoom 3.84. **E.** Topographical (3D) profilometric image of TiCP Osseotite® surface by confocal microscopy. Peaks, black arrow, valleys, white arrow.

F. Topographical (2D) reconstruction of a 3D series obtained with the CLSM, showing the distribution of stress fibers (green), mainly in the filopodia (black star) and lamellipodia (white star), that are oriented to the focal adhesion sites in a NHOst cell growing on the rough Osseotite® surface (mixed red). Peaks, black arrow, valleys, white arrow. x 63. Zoom 1.

Microtopography and cytoskeleton

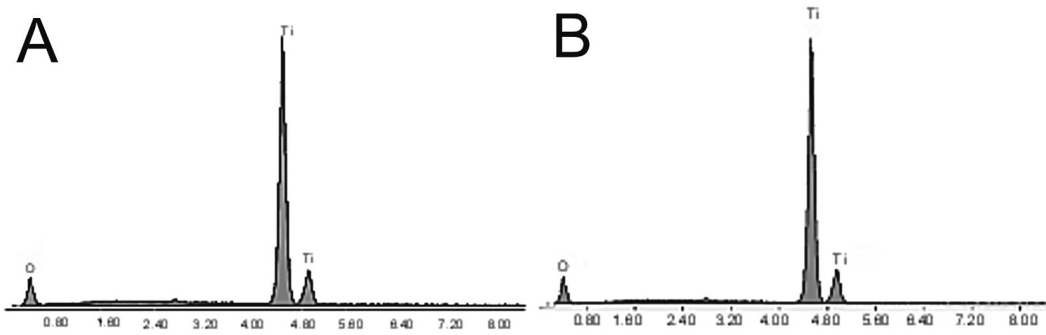


Fig. 4. Spectra obtained by scanning electron microscopy and energy dispersive X-ray microanalysis, which identified Ti and O peaks. **A.** Spectra for Ti CP machined disks. **B.** Spectra for Ti CP Osseotite® disks. Spectra were acquired during 200 sec., at 20.00 kV

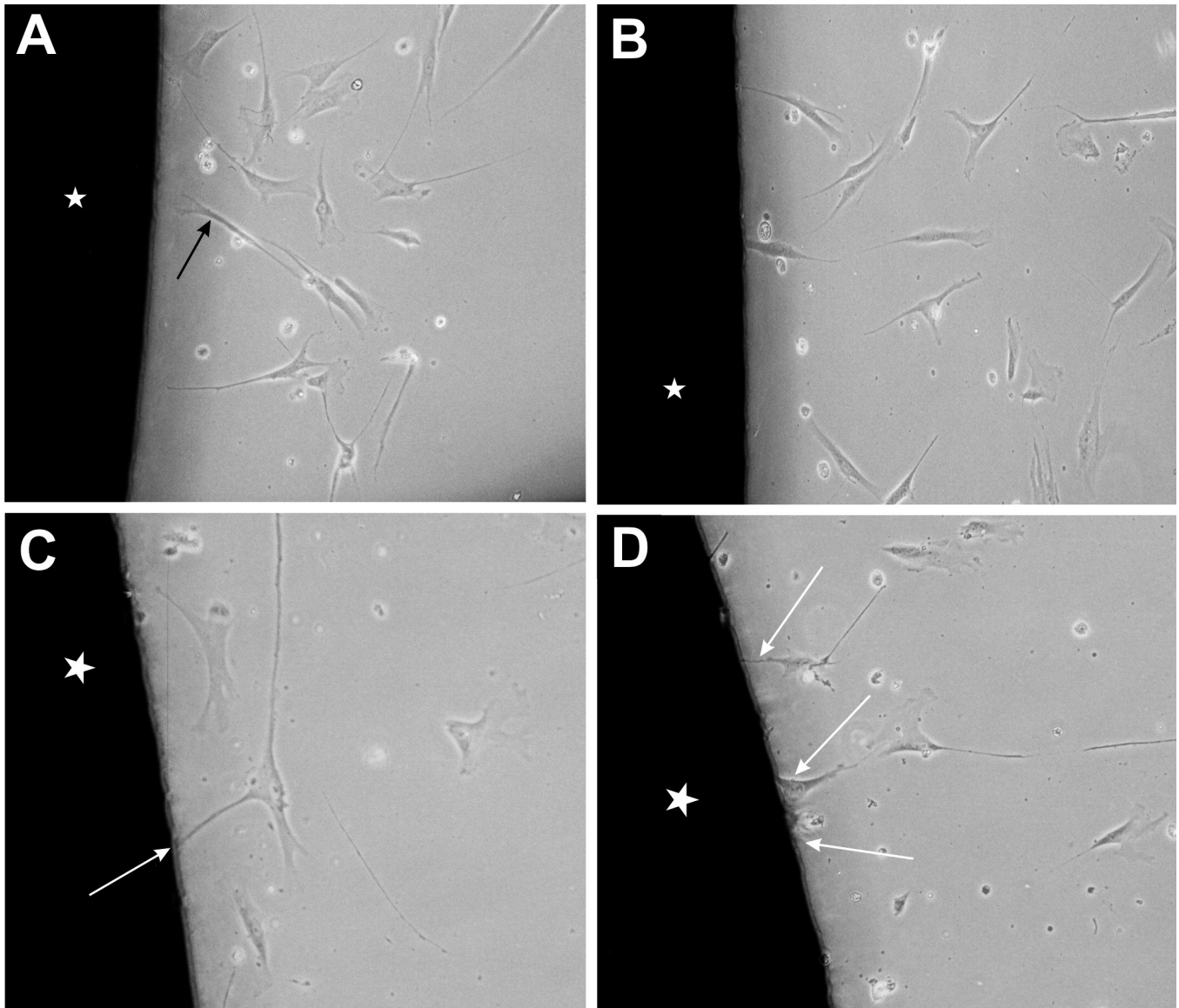


Fig. 5. A. Phase 1, In the first minutes, in the presence of TICP Osseotite® disks (white star) cells (marked with black arrow) started flattening, induced by electrostatic forces and passive bindings ligand-receptor in the initial phase of the adhesion process adsorbing to proteins on the disk surface. **B.** After 10 minutes, the alignment phase becomes evident with most of the cells facing the disk (white star). **C.** Dispersion phase with cells along the disk surface (white star), with active cell participation, cytoskeletal reorganization, bindings and initial establishment of focal adhesions (white arrow marks cell-surface contact). **D.** Finally, cells (marked with white arrows) clearly establish focal adhesions with the disk surface (*). All images were obtained in the phase contrast microscope, at a magnification of x 40. Zoom 2.0

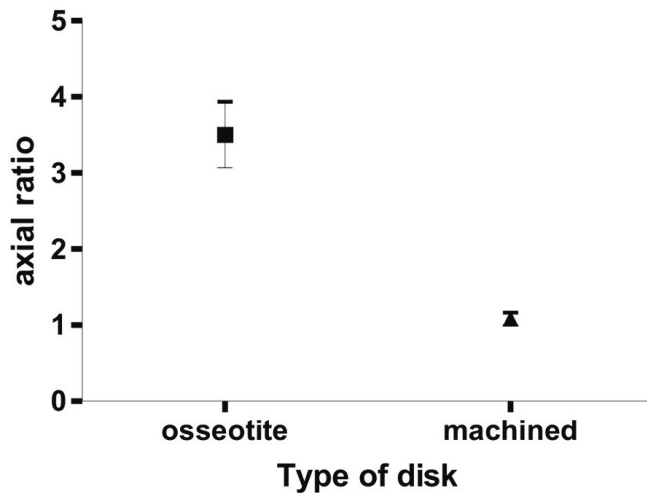


Fig. 6. Axial ratio for cells grown on TiCP Osseotite and TiCP machined disks were found to be statistically different ($p: 0.02$).

distinct morphologies depending on the architectural features of their substrate. Comparison of the general morphology of the spreading cells indicated that in the machined TiCP disks, as long as the peak to peak distance is less than the length of the cell body, the cells flattened and spread adopting a morphology largely radial, with a mean axial ratio of 1.1 (Fig. 6) and anchored themselves to the surface through long dendritic filopodia both along the grooves of the surface or crossing over them in a perpendicular way (Fig. 2A, B, a,b, C). In the TiCP Osseotite[®], where the distance between peaks increases, the cells presented an increasingly polarised spreading with emission of either wide lamellopodia or long filopodia, depending on the surface roughness and the distance between subadjacent peaks, and showed the longest morphology, with a mean axial ratio that rose to 3.5. (Fig. 3A,B) Comparison of axial ratios revealed a significant difference between cell growth on both surfaces ($p: 0.02$). (Fig. 6). The projected area of the cell was also strongly affected by the surface patterns, reaching highest values when spreading occurred in all directions and decreasing when it was restricted to one direction primarily.

Cytoskeletal organization

In cells spreading over Ti CP machined surface stress fibers were observed running in all directions, as confirmed by the topographical study (Fig. 2F), often crossing several rings, by extending lamellopodia and filopodia over them, containing actin microfilaments. In the oriented cells the cytoskeleton was also aligned in the direction of the grooves (Fig. 3A-D).

In cells spread over TiCP Osseotite[®], the actin cytoskeleton adopted a quite different organisation, characterised by actin bundles running either perpendicularly or slightly obliquely with a “segmented”

structure, with apparently segmented contractile units defined topographically by the anchorage points organized according to the surface structure. (Fig. 3A,B,F) Parallel actin filaments were observed along the cellular processes with anchoring to focal contacts found on relative topographical peaks. (Fig. 3C,D)

Discussion

Biomaterials currently available for clinical use are known for their good biocompatibility. However if most of them have the mechanical properties required for a defined implantation, they do not all possess the necessary bioactivity properties for good tissue regeneration.

For a better understanding of the process by which microtopography modulates osteoblastic cell adhesion, in the present study we have developed an *in vitro* model using the human osteoblastic cell line NHOst[®] to study actin cytoskeletal organization during the initial phases of the adhesion process to two different titanium implant surfaces, TiCP machined and dual thermo-acid etching Ti CP Osseotite[®] prepared as disks for *in vitro* manipulation.

Surface quality is one of many factors that contributes to the success of implants (Boyan et al., 2003; Torensma et al., 2003; Keselowsky et al., 2004; Lüthen et al., 2005; Sader et al., 2005). By using SEM and x-ray microanalysis we have determined the exact disk composition, only titanium and oxygen in both types of disks, as a result of the oxidation process, and also discarded contamination by cytotoxic compounds. This data contributed to demonstrate the accuracy of the fabrication process, together with topographical study of the surfaces. The use of CLSM confirmed SEM observed topographical differences between the TiCP machined, planar, and TiCP Osseotite[®], rough, surfaces. This fact enforces the importance of CLSM, which allows the combined reflection and fluorescence study, for an accurate assessment of cell behaviour with respect to different scaffolds.

The use of glycerol/water immersion objective with a long working distance and the simultaneous detection of the fluorescence and the reflection channels, in the present work, has demonstrated to be a valuable tool for the assessment of the interaction between cells and scaffolds and the subsequent achievement of the most favourable conditions for the non-invasive analysis of osteoblasts-implants interface by CLSM, thus allowing us to obtain a 3D view of fluorescent labelled cell cytoskeleton at the cell implant interface. The results demonstrate that the methodology employed is mandatory for a proper approach to the study of the mechanisms of cell-surface interactions.

In our model, we have used a human normal osteoblastic cell line, NHOst, with highly specific requirements for cell seeding density, optimal medium and specific supplements for their growth, daily changed, and control of confluence. Cell passages

ranging from two to nine were used for the experimental design. The use of human normal osteoblasts is an important requirement in order to reproduce, as much as possible, the biomedical conditions on which implant devices should be osseointegrated. According to our findings, osteoblasts are able to actively adhere and spread onto the tested surfaces. However, their adhesion and spreading were dependent on surface microtopography, thus determining the initial cellular events at the cell-material interface (Anselme, 2000), as we have observed with the phase contrast examination from the initial phases of adhesion process.

Rough surfaces have been described to be important for initial osteogenesis inducing the healing of the wound and consequently osseointegration, at least during unloaded conditions, when compared to smooth surfaces. It is possible that the increased degree of bone implant contact may increase the loadbearing capacity. Rough surfaces can be a determining factor for prognosis and success of implants (Shah et al., 1999; Anselme, 2000; Ivanoff et al., 2001; Jayaraman et al., 2003; Papalexioiu et al., 2004; Zimmerman et al., 2004).

Our results show that the osteoblastic adhesion is significantly different on the two commonly and successfully used orthopaedic biomaterials. In smooth surfaces, Ti CP machined, predominantly planar bone cells with an axial ratio of 1.1, were randomly oriented, with stress fibers running in all directions, although they were aligned parallel to the direction of the grooves, and thin filopodia, fundamentally determined by the presence of the striated surface of the rings as described above, in a similar fashion to that described by Zimmerman on patterned glass surfaces consisting of 2 μm -wide, parallel adhesive stripes coated with fibronectin (Zimmerman et al., 2004; Sader et al., 2005).

In contrast, on TiCP Osseotite[®] surfaces the osteoblastic cells are able to conform to the irregular terrain of the substrate with focal adhesions only established on the relative topographical peaks evenly distributed and separated for a longer distance than in the machined surface. This process results in the more elongated morphology observed in cells cultured on TiCP Osseotite[®] surfaces, with a mean axial ratio of 3.5. Clearly defined wide lamellopodia and long filopodia, in which the cells typically displayed enhanced expression of stress fibers, appeared to be able to form large clear focal contacts with the rough surface. The enhanced degree of cytoskeletal organization of cells cultured on rough titanium (TiCP Osseotite[®]) in a segmented structure with apparently separated contractile units supports an active role for the biomaterial surface in the events that govern osteoblastic cell maturation. The architecture of actin cytoskeleton is essential for the maintenance of cell shape and cell adhesion. If assembling in long bundles, F-actin supports finger-like protrusions of the plasma membrane known as filopodia; if assembled in the form of a branched array, it supports sheet-like protrusions known as lamellipodia. If preset in bundles coupled with adhesion plaques, actin “stress

fibers” may transmit forces to the substrate (Zigmond, 1996; Shat et al., 1999; Anselme, 2000; Pierres et al., 2002; Boyan et al., 2003; Bächle and Kohal, 2004; Jayaraman et al., 2004; Veis et al 2004; Dalby et al., 2006).

The results presented herein enforce the role of the rough substrate surface in affecting osteoblastic cell adhesion and provide valuable information for the design of material surfaces that are required for the development of an appropriate osteogenic surface for osteoblastic anchorage and maturation compared to machined surface in dental implants. This report using normal human osteoblastic cells indicates that these cells are especially sensitive to nanocues through filopodial production that enhances the necessary adhesion required for a successful osseointegration.

Acknowledgements. This work has been supported by a FIS 05/1816 grant from Instituto de Salud Carlos III, Spain. The authors want to acknowledge 3i (Palm Beach Gardens, USA) for prefabricating and kindly providing the titanium disks.

References

- Al-Nawas B. and Gotz H. (2003). Three-dimensional topographic and metrologic evaluation of dental implants by confocal laser scanning microscopy. *Clin. Implant Dent. Relat. Res.* 5, 176-183.
- Anselme K. (2000). Osteoblast adhesion on biomaterials. *Biomaterials* 21, 667-681.
- Bächle M. and Kohal R.J. (2004). A systematic review of the influence of different titanium surfaces on proliferation, differentiation and protein synthesis of osteoblast-like MG63 cells. *Clin. Oral Implants Res.* 15, 683-692.
- Boyan B.D., Lossdorfer S., Wang L., Zhao G., Lohmann C.H., Cochran D.L. and Schwartz Z. (2003). Osteoblasts generate an osteogenic microenvironment when grown on surfaces with rough microtopographies. *Eur. Cell Mater.* 24, 22-27.
- Brånemark P.I., Adell R., Albrektsson T., Lekholm U., Lundkvist S. and Rockler B. (1983). Osseointegrated titanium fixtures in the treatment of edentulousness. *Biomaterials* 4, 25-28.
- Dalby M.J., McCloy D., Robertson M., Agheli H., Sutherland D., Affrossman S. and Oreffo R.O. (2006). Osteoprogenitor response to semi-ordered and random nanotopographies. *Biomaterials* 27, 2980-2987.
- Diener A., Nebe B., Luthen F., Becker P., Beck U., Neumann H.G. and Rychly J. (2005). Control of focal adhesion dynamics by material surface characteristics. *Biomaterials* 26, 383-392.
- Ivanoff C.J., Hallgren C., Widmark G., Sennerb L. and Wennerberg A. (2001). Histologic evaluation of the bone integration of TiO(2) blasted and turned titanium microimplants in humans. *Clin. Oral Implant Res.* 12, 128-134.
- Jayaraman M., Meyer U., Buhner M., Joos U. and Wiesmann H.P. (2004). Influence of titanium surfaces on attachment of osteoblast-like cells in vitro. *Biomaterials* 25, 625-631.
- Keselowsky B.G., Collard D.M. and Garcia A.J. (2004). Surface chemistry modulates focal adhesion composition and signaling through changes in integrin binding. *Biomaterials* 25, 5947-5954.
- Ku C.H., Pioletti D.P., Browne M. and Gregson P.J. (2002). Effect of

- different Ti-6Al-4V surface treatments on osteoblasts behaviour. *Biomaterials* 23,1447-1454.
- Lange R., Luthen F., Beck U., Rychly J., Baumann A. and Nebe B. (2002). Cell-extracellular matrix interaction and physico-chemical characteristics of titanium surfaces depend on the roughness of the material. *Biomol. Eng.* 19, 255-261.
- Lenhart S., Meier M.B., Meyer U., Chi L. and Wiesmann H.P. (2005). Osteoblast alignment, elongation and migration on grooved polystyrene surfaces patterned by Langmuir-Blodgett lithography. *Biomaterials* 26, 563-570.
- Linez-Bataillon P., Monchau F., Bigerelle M. and Hildebrand H.F. (2002). In vitro MC3T3 osteoblast adhesion with respect to surface roughness of Ti6Al4V substrates. *Biomol. Eng.* 19, 133-141.
- Lüthen F., Lange R., Becker P., Rychly J., Beck U. and Nebe J.G. (2005). The influence of surface roughness of titanium on beta1- and beta3-integrin adhesion and the organization of fibronectin in human osteoblastic cells. *Biomaterials* 26, 2423-2440.
- Mustafa K., Wennerberg A., Wroblewski J., Hultenby K., Lopez B.S. and Arvidson K. (2001). Determining optimal surface roughness of TiO₂ blasted titanium implant material for attachment, proliferation and differentiation of cells derived from human mandibular alveolar bone. *Clin. Oral Implants Res.* 12, 15-25.
- Papalexiou V., Novaes A.B. Jr, Grisi M.F., Souza S.S, Taba M. Jr. and Kajiwara J.K. (2004). Influence of implant microstructure on the dynamics of bone healing around immediate implants placed into periodontally infected sites. A confocal laser scanning microscopic study. *Clin. Oral Implants Res.* 15, 44-53.
- Pierres A., Benoliel A.M. and Bongrand P. (2002). Cell fitting to adhesive surfaces: A prerequisite to firm attachment and subsequent events. *Eur. Cell Mater.* 3, 31-45.
- Rodriguez-Rius D. and Garcia-Saban F.J. (2005). Physico-chemical characterization of the surface of 9 dental implants with 3 different surface treatments. *Med. Oral Patol. Oral Cir. Bucal.* 10, 58-62
- Ronold H.J., Ellingsen J.E. and Lyngstadaas S.P. (2003a). Tensile force testing of optimized coin-shaped titanium implant attachment kinetics in the rabbit tibiae. *J. Mater. Sci. Mater. Med.* 14, 843-849.
- Ronold H.J., Lyngstadaas S.P. and Ellingsen J.E. (2003b). A study on the effect of dual blasting with TiO₂ on titanium implant surfaces on functional attachment in bone. *J. Biomed. Mater. Res.* 67, 524-530.
- Sader M.S., Balduino A., de Almeida Soares G. and Borojevic R. (2005). Effect of three distinct treatments of titanium surface on osteoblast attachment, proliferation, and differentiation. *Clin. Oral Implants Res.* 16, 667-675.
- Shah A.K., Sinha R.K., Hickok N.J. and Tuan R.S. (1999). High-resolution morphometric analysis of human osteoblastic cell adhesion on clinically relevant orthopedic alloys. *Bone* 245, 499-506.
- Torensma R., ter Brugge P.J, Jansen J.A. and Figdor C.G. (2003). Ceramic hydroxyapatite coating on titanium implants drives selective bone marrow stromal cell adhesion. *Clin. Oral Implants Res.* 14, 569-577.
- Veis A.A., Trisi P., Papadimitriou S., Tsirlis A.T., Parissis N.A., Desiris A.K. and Lazzara R.J. (2004). Osseointegration of Osseotite and machined titanium implants in autogenous bone graft. A histologic and histomorphometric study in dogs. *Clin. Oral Implants Res.* 15, 54-61.
- Zigmond S.H. (1996). Signal transduction and actin filament organization. *Curr. Opin. Cell Biol.* 8, 66-73.
- Zimmerman B., Arnold M., Ulmer J., Blummel J., Besser A., Spatz J.P. and Geiger B. (2004). Formation of focal adhesion-stress fibre complexes coordinated by adhesive and non-adhesive surface domains. *IEE Proc. Nanobiotechnol.* 151, 62-66.
- Zreiqat H., Valenzuela S.M., Nissan B.B., Roest R., Knabe C., Radlanski R.J., Renz H. and Evans P.J. (2005). The effect of surface chemistry modification of titanium alloy on signalling pathways in human osteoblasts. *Biomaterials* 26, 7579-7586.